Angewandte Chemie
Eine Zeitschrift der Gesellschaft Deutscher Chemiker

Supporting Information

The Mystery of the Benzene-Oxide/Oxepin Equilibrium—Heavy-Atom Tunneling Reversed by Solvent Interactions

Tim Schleif[+], *Melania Prado Merini*[+], *and Wolfram Sander**

anie_202010452_sm_miscellaneous_information.pdf

Supporting Information

Contents

IR spectroscopic data

Methodology

Matrix isolation experiments were performed by standard techniques using two-staged closed-cycle helium cryostats (cooling power 1 W at 4 K) to obtain temperatures around 3 K. The

matrices were generated by co-deposition of the mixture of **1** and **2** with a large excess of argon (doped with 1% of H_2O or ICF_3) on top of a cold CsI window at 3 K. FTIR spectra were recorded in the range between 400 and 4000 cm^{-1} with 0.5 cm^{-1} resolution, often passing the IR beam of the spectrometer through an IR long pass interference filter (passing ≥ 2200 cm^{-1}).

Table S1. IR spectroscopic data of benzene oxide **1**.

Mode	DFT[a] $\tilde{\nu}$/cm^{-1} (I_{abs})	CC[b] $\tilde{\nu}$/cm^{-1} (I_{abs})	Argon[c] $\tilde{\nu}$/cm^{-1} (I_{rel})	Assignment[d]
26	1640 (2)	1601 (2)	1555 (1)	C=C stretch
25	1477 (10)	1465 (12)	1434 (13)	C=C stretch
24	1440 (3)	1425 (4)	1397 (4)	C-H scis.
23	1414 (5)	1394 (4)		C-H scis. + C-O stretch.
21	1287 (13)	1264 (8)	1213 (2)	C-H scis. + C-O stretch.
20	1211 (1)	1202 (1)	1183 (1)	C-H rock.
19	1196 (5)	1186 (5)	1164 (6)	C-H scis.
17	1079 (12)	1065 (14)	1046 (11)	C-H scis. + C-O stretch.
16	1037 (20)	1007 (29)	988 (18)	C-H scis.
15	1027 (8)	988 (10)	967 (8)	C-H rock.
13 (14)	995 (2)	968 (5)	953 (4)	C-H wag.
12 (13)	980 (5)	955 (10)		
11 (12)	954 (16)	931 (19)	921 (9)	C-H wag. + C-O stretch.
9	805 (72)	791 (100)	772 (100)	C-H wag. + C-O stretch.
7	725 (21)	703 (30)	691 (25)	C-H scis. + C-O stretch.
5 (6)	633 (12)	600 (20)	610 (9)	C-C stretch.
3	467 (12)	459 (18)	456 (11)	C-H wag.

[a] Calculated at M06-2X-D3/def2-TZVP level of theory. [b] Calculated at CCSD(T)/def2-TZVP level of theory. [c] Argon matrix at 3 K. [d] Tentative assignment.

Table S2. IR spectroscopic data of oxepin **2**.

Mode	DFT[a] $\tilde{\nu}$/cm^{-1} (I_{abs})	CC[b] $\tilde{\nu}$/cm^{-1} (I_{abs})	Argon[c] $\tilde{\nu}$/cm^{-1} (I_{rel})	Assignment[d]
26	1700(20)	1658 (23)	1614 (17)	C=C stretch
21	1281 (52)	1272 (50)	1242 (42)	C-H scis. + C-O stretch.
20	1239 (5)	1228 (6)	1206 (5)	C-H scis.
18	1116 (63)	1101 (70)	1079 (81)	C-H rock.
16 (17)	1011 (11)	988 (12)	971 (12)	C-H rock.
12	945 (4)	916 (5)	903 (6)	C-C stretch.
11	921 (2)	895 (2)	893 (5)	C-H rock.
10	853 (7)	834 (7)	831 (8)	C-H wag.
9 (8)	787 (25)	758 (25)	751 (17)	C-H wag.
7	771 (95)	752 (100)	738 (100)	C-H wag.

[a] Calculated at M06-2X-D3/def2-TZVP level of theory. [b] Calculated at CCSD(T)/def2-TZVP level of theory. [c] Argon matrix at 3 K. [d] Tentative assignment.

Table S3. IR spectroscopic data of complex **1**··ICF_3.

Mode	*endo*-**1**··ICF_3 [a] $\tilde{\nu}$/cm^{-1} (I_{abs})	*exo*-**1**··ICF_3 [a] $\tilde{\nu}$/cm^{-1} (I_{abs})	Ar/1% ICF_3[b] $\tilde{\nu}$/cm^{-1} (I_{rel})	Assignment[c]

40	1476 (11)	1477 (13)	1433 (7)	C-C stretch.
39	1439 (5)	1440 (5)	1398 (4)	C-H scis.
35	1228 (243)	1234 (243)	1150 (76)	C-F stretch.
34	1225 (242)	1231 (243)		
30	1124 (659)	1123 (672)	1081 (100)	C-I stretch.
28	1036 (40)	1034 (40)	984 (15)	C-H wag.
23	954 (34)	955 (18)	919 (16)	C-H wag. + C-O stretch.
21	806 (90)	808 (70)	773 (64)	C-H wag. + C-O stretch.
18	724 (13)	726 (52)	686 (15)	C-H scis. + C-O stretch.

[a] Calculated at M06-2X-D3/def2-TZVP level of theory. [b] Argon matrix doped with 1% ICF_3 at 3 K. [c] Tentative assignment.

Table S4. IR spectroscopic data of complex **2**··ICF_3.

Mode	*endo*-**2**··ICF_3 [a] $\tilde{\nu}$/cm^{-1} (I_{abs})	*exo*-**2**··ICF_3 [a] $\tilde{\nu}$/cm^{-1} (I_{abs})	Ar/1% ICF_3 [b] $\tilde{\nu}$/cm^{-1} (I_{rel})	Assignment[c]
42	1730 (19)	1733 (28)	1634 (6)	C=C stretch.
41	1707 (17)	1708 (19)	1615 (10)	
40	1665 (6)	1664 (12)		
36	1275 (43)	1271 (53)	1231 (32)	C-H scis.
33/35	1231 (242)	1237 (247)	1165 (100)	C-F stretch.
32/34	1228 (243)	1236 (239)		
31	1122 (661)	1124 (711)	1067 (86)	C-I stretch.
28	1013 (22)	1007 (40)	972 (15)	C-C wag.
24	979 (14)	947 (18)	910 (21)	C-C stretch.
19/18	774 (99)	765 (109)	738 (88)	C-H wag.

[a] Calculated at M06-2X-D3/def2-TZVP level of theory. [b] Argon matrix doped with 1% ICF_3 at 3 K. [c] Tentative assignment.

Table S5. IR spectroscopic data of complex **1**··H_2O.

Mode	*endo*-a-**1**·· H_2O [a] $\tilde{\nu}$/cm^{-1} (I_{abs})	*endo*-b-**1**·· H_2O [a] $\tilde{\nu}$/cm^{-1} (I_{abs})	*exo*-**1**·· H_2O [a] $\tilde{\nu}$/cm^{-1} (I_{abs})	Ar/1% H_2O [b] $\tilde{\nu}$/cm^{-1} (I_{rel})	Assignment[c]
31	1477 (13)	1473 (11)	1477 (13)	1435 (15)	C-C stretch.
29	1413 (7)	1408 (7)	1411 (3)	1398 (5)	C-H scis.
27	1288 (14)	1286 (15)	1291 (16)	1247 (5)	C-H wag.
25	1201 (5)	1191 (5)	1196 (6)	1166 (10)	C-H rock.
22	1037(26)	1033 (26)	1033 (23)	984 (31)	C-H wag.
17	958 (20)	954 (19)	956 (17)	918 (46)	C-H wag. + C-O stretch.
15	809 (77)	806 (73)	811 (74)	919 (16)	C-H wag. + C-O stretch.
13	724 (16)	721 (21)	724 (29)	773 (64)	C-H wag. + C-O stretch.

[a] Calculated at M06-2X-D3/def2-TZVP level of theory. [b] Argon matrix doped with 1% H_2O at 3 K. [c] Tentative assignment.

Table S6. IR spectroscopic data of complex **2**··H_2O.

Mode	*endo*-a-**2**·· H_2O [a] $\tilde{\nu}$/cm^{-1} (I_{abs})	*endo*-b-**2**·· H_2O [a] $\tilde{\nu}$/cm^{-1} (I_{abs})	*exo*-**2**·· H_2O [a] $\tilde{\nu}$/cm^{-1} (I_{abs})	Ar/1% H_2O [b] $\tilde{\nu}$/cm^{-1} (I_{rel})	Assignment[c]
27	1276 (49)	1271 (43)	1270 (43)	1233 21)	C=C stretch.
24	1113 (61)	1111 (58)	1106 (62)	1070 (50)	C=C stretch.
19	973 (4)	976 (5)	972 (4)	1010 (1)	C-H wag.
16	852 (7)	849 (9)	850 (7)	831 (2)	C-H wag..
14	784 (9)	778 (8)	785 (2)	752(10)	C-H wag. + C-O stretch.

[a] Calculated at M06-2X-D3/def2-TZVP level of theory. [b] Argon matrix doped with 1% H_2O at 3 K. [c] Tentative assignment.

Table S7. IR spectroscopic data of 2-oxabicyclo[3.2.0]hepta-3,6-diene.

Mode	DFT[a] $\tilde{\nu}$/cm^{-1} (I_{abs})	Argon[b] $\tilde{\nu}$/cm^{-1} (I_{rel})	Assignment[c]
24	1342 (36)	1300 (76)	C-H rock. + C-C stretch.
20	1218 (12)	1178 (26)	C-H scis.
19	1182 (68)	1140 (100)	C-H scis. + C-O stretch.
18	1140 (6)	1099 (27)	C-H scis. + C-C stretch.
17	1095 (41)	1044 (23)	C-H scis. + C-O stretch.
16	1044 (9)	1012 (25)	C-H scis.
14	998 (42)	942 (86)	C-C stretch. + C-O stretch.
9	887 (17)	860 (55)	C-H wag.
6	729 (34)	706 (58)	C-H wag.

[a] Calculated at M06-2X-D3/def2-TZVP level of theory. [b] Argon matrix at 3 K. [c] Tentative assignment.

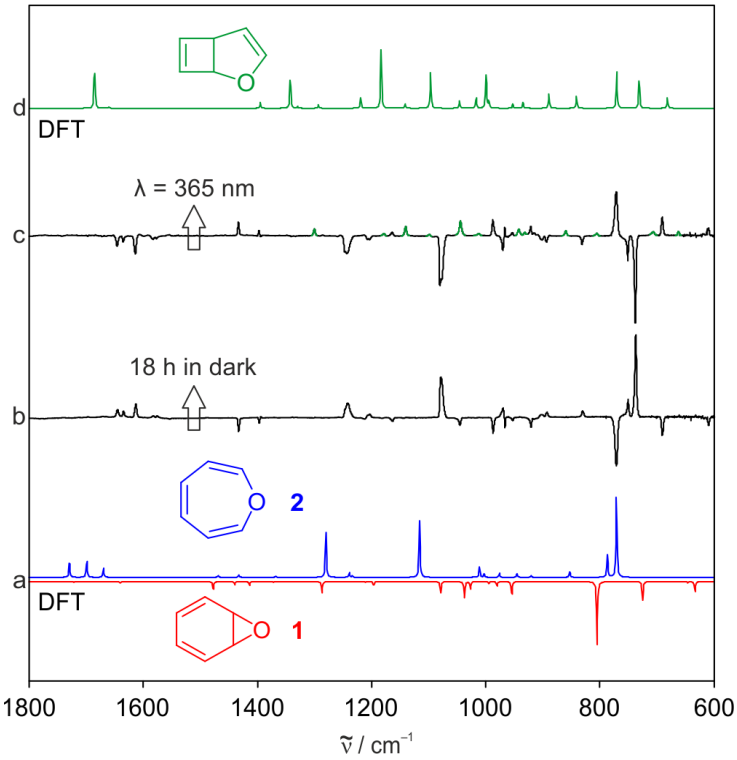

Figure S1. Heavy-atom tunneling and photochemical interconversion of valence tautomers of C_6H_6O. a) Theoretical IR spectra of **1** (pointing downwards) and **2** (pointing upwards). b) IR difference spectrum obtained after keeping an argon matrix containing **1** and **2** in the dark at 3 K for 18 h. c) IR difference spectrum obtained after irradiation of the matrix with λ = 365 nm at 3 K for 30 min. Peaks highlighted in green are not affected by keeping the matrix in the dark. d) Theoretical IR spectrum of 2-oxabicyclo[3.2.0]hepta-3,6-diene. All calculations were performed at the M06-2X-D3/def2-TZVP level of theory.

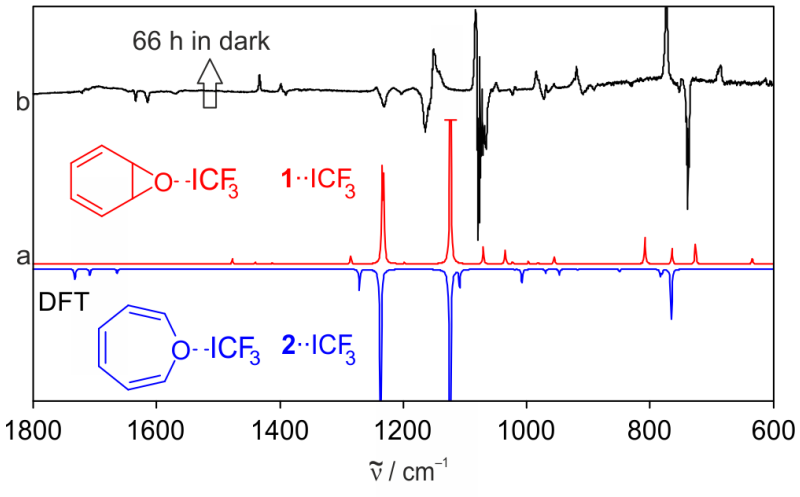

Figure S2. Heavy-atom tunneling in the interconversion of complexes **1**··ICF_3 and **2**··ICF_3. a) Theoretical IR spectra of **1**··ICF_3 (pointing downwards) and **2**··ICF_3 (pointing upwards). For simplicity, the *exo*-complexes were chosen as representatives; the *endo*-complexes only exhibit marginal shifts in wavelength as seen in Tables S3+4. b) IR difference spectrum obtained after keeping an argon matrix containing **1**··ICF_3 and **2**··ICF_3 in the dark at 3 K for 66 h.

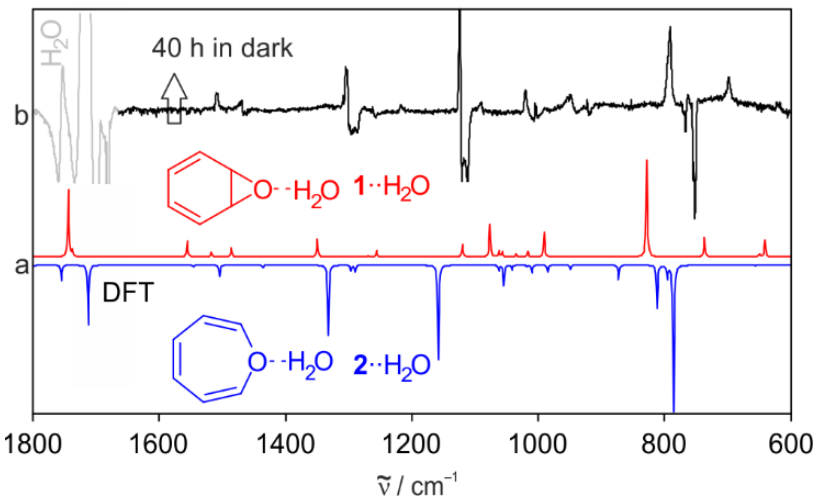

Figure S3. Heavy-atom tunneling in the interconversion of complexes **1**··H_2O and **2**··H_2O. a) Theoretical IR spectra of **1**··H_2O (pointing downwards) and **2**··H_2O (pointing upwards). For simplicity, the *endo*-b complexes were chosen as representatives; the *endo*-a and .*exo*. complexes only exhibit marginal shifts in wavelength as seen in Tables S5+6. b) IR difference spectrum obtained after keeping an argon matrix containing **1**·· H_2O and **2**·· H_2O in the dark at 3 K for 40 h.

Experimental kinetic data

Methodology

In order to determine the rate constants, the decreasing intensity of the peak at 772 cm^{-1} belonging to **1** and the increasing intensities at 737 and 1078 cm^{-1} assigned to **2** were continuously monitored and fitted to Eq. 1. In case of ICF_3 doped matrices, the integrated increasing peaks were 686 and 773 cm^{-1} (assigned to **1**··ICF_3) and the decreasing ones at 1615 and 1634 cm^{-1} (assigned to **2**··ICF_3). In the H_2O doped matrices the integrated peaks were two increasing at 773 and 984 cm^{-1} (assigned to **1**··H_2O) and a decreasing one at 738 cm^{-1} (assigned to **2**··H_2O). This equation[1] takes into account the presence of multiple matrix sites in the rigid argon matrix whose varying sizes and geometries result in a range of rate constants, represented by the dispersion coefficient β; the addition of c allows for a simultaneous fit of increasing and decreasing peak intensities. By means of reverting the ring expansion of **1** to **2** via irradiation with λ = 365 nm, the kinetics of this reaction could be investigated in the same matrix at different temperatures.

$$I = I_0 \cdot e^{-(kt)^{\beta}} + c \qquad \text{with } 0 < \beta < 1 \qquad \text{(eq. 1)}$$

Apparent half-lives (τ_{app}) can be calculated for these kinetics via Equation (2) though the high dispersivity of these kinetics mean that these "half-lives" have to be considered rough approximations.

$$\frac{\sqrt[\beta]{ln\ 2}}{k} = \tau_{app} \qquad \text{(eq. 2)}$$

For the evaluation of the kinetics of the complexated molecules, the intensities of the corresponding peaks (with slights shift in frequencies) were fitted. Kinetic measurements could be performed multiple times within the same matrix by reversion of the tunneling reaction via irradiation with λ = 254 nm or by additional complex formation via repeated annealing.

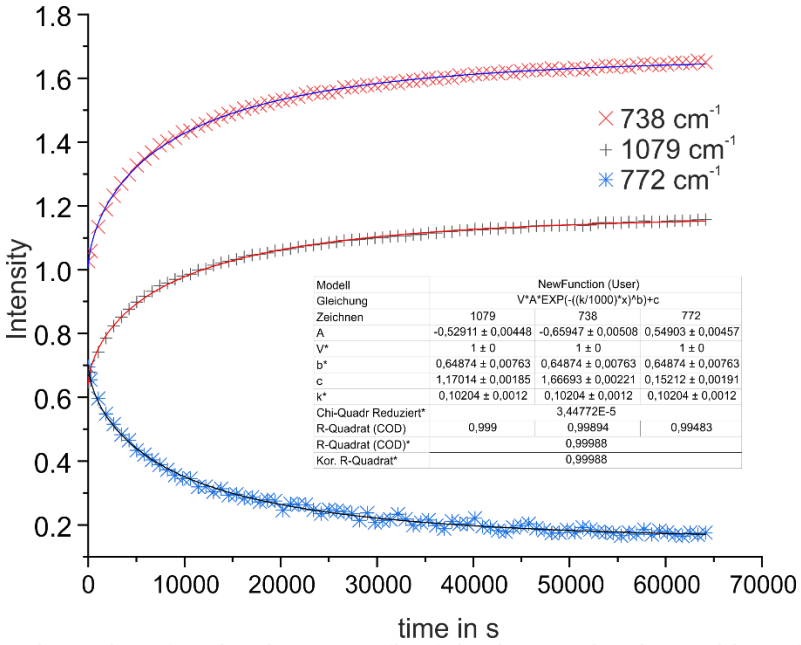

Figure S3. Examplary plot of a simultaneous fit of the increasing intensities of the IR peaks at 737 and 1078 cm^{-1} as well as the decreasing intensity of the IR peak at 772 cm^{-1} to eq. 1 as recorded for an argon matrix at 3 K.

Table S4. Rate constants k and (apparent) half-lives τ_{app} as fitted to Equation (1) with β as a variable, for the ring expansion of benzene oxide (**1**) to oxepin (**2**) in an argon matrix. The duration of the experiment is given as t_{final}. Most measurements (for exceptions, s. notes) were performed using a filter with a cutoff of $\tilde{\nu}$ > 2000 cm^{-1}.

T / K	k / 10^{-5} s^{-1}	τ_{app} / h	t_{final} / h	β
3[a,b]	5.6 ± 1.2	3.3	17	0.9
3[a,b]	5.1 ± 0.1	3.2	72	0.7
3	4.7 ± 0.2	2.8	23	0.5
6	2.4 ± 0.3	6.3	25	0.6
10	2.7 ± 0.6	4.9	21	0.5
15	1.4 ± 0.4	9.5	21	0.5
20	2.0 ± 0.2	7.5	25	0.6
25	1.0 ± 0.4	13.3	26	0.5

[a] Measurement was performed without using a filter. [b] Measurement was performed directly after deposition.

Table S5. Rate constants k and (apparent) half-lives τ_{app} as fitted to Equation (1) with β = 0.6, for the ring expansion of benzene oxide (**1**) to oxepin (**2**) in an argon matrix. The duration of the experiment is given as t_{final}. Most measurements (for exceptions, s. notes) were performed using a filter with a cutoff of $\tilde{\nu}$ > 2000 cm^{-1}.

T / K	k / 10^{-5} s^{-1}	τ_{app} / h	t_{final} / h
3[a,b]	3.5 ± 1.9	4.3	17
3[a,b]	5.9 ± 0.2	2.6	72
3	5.4 ± 0.2	2.8	23
3[c]	5.3 ± 1.7	-	-
6	2.2 ± 0.2	6.9	25
10	3.8 ± 0.3	4.0	21
15	2.3 ± 0.2	6.6	21
20	2.3 ± 0.1	6.6	25
25	1.7 ± 0.2	8.9	26

[a] Measurement was performed without using a filter. [b]

Measurement was performed directly after deposition. [c] Weighted mean and standard error.

Table S6. Rate constants k and (apparent) half-lives τ_{app} as fitted to Equation (1) with β as a variable, for the ring contraction of complexated oxepin (**2**··ICF_3) to complexated benzene oxide (**1**··ICF_3) in an argon matrix doped with 1% of ICF_3. The duration of the experiment is given as t_{final}. All measurements were performed using a filter with a cutoff of $\tilde{\nu}$ > 2000 cm^{-1}.

T / K	k / 10^{-5} s^{-1}	τ_{app} / h	t_{final} / h	β
3	4.0 ± 0.1	3.3	66	0.5
3	3.0 ± 0.1	4.4	83	0.5
3	2.4 ± 0.1	5.6	42	0.5

Table S7. Rate constants k and (apparent) half-lives τ_{app} as fitted to Equation (1) with β = 0.5, for the ring contraction of complexated oxepin (**2**··ICF_3) to complexated benzene oxide (**1**··ICF_3) in an argon matrix doped with 1% of ICF_3. The duration of the experiment is given as t_{final}. All measurements were performed using a filter with a cutoff of $\tilde{\nu}$ > 2000 cm^{-1}.

T / K	k / 10^{-5} s^{-1}	τ_{app} / h	t_{final} / h
3	4.0 ± 0.1	3.3	66
3	3.0 ± 0.1	4.4	83
3	2.4 ± 0.1	5.6	42
3[a]	3.1 ± 0.4	-	-

[a] Weighted mean and standard error.

Table S8. Rate constants k and (apparent) half-lives τ_{app} as fitted to Equation (1) with β as a variable, for the ring contraction of complexated oxepin (**2**··H_2O) to complexated benzene oxide (**1**··H_2O) in an argon matrix doped with 1% of H_2O. The duration of the experiment is given as t_{final}.

T / K	k / 10^{-5} s^{-1}	τ_{app} /h	t_{final} / h	β
3	5.3 ± 0.1	2.5	43	0.5
3	3.0 ± 0.1	4.4	43	0.5
3[a]	2.7 ± 1.3	4.9	40	0.5

[a] Measurement was performed using a filter with a cutoff of $\tilde{\nu}$ > 2000 cm^{-1}.

Table S9. Rate constants k and (apparent) half-lives τ_{app} as fitted to Equation (1) with $\beta = 0.5$, for the ring contraction of complexated oxepin (**2**··H_2O) to complexated benzene oxide (**1**··H_2O) in an argon matrix doped with 1% of H_2O. The duration of the experiment is given as t_{final}.

T / K	k / 10^{-5} s^{-1}	τ_{app} /h	t_{final} / h
3	5.4 ± 0.1	2.5	43
3	3.0 ± 0.1	4.4	43
3[a]	2.6 ± 1.1	5.1	40
3[b]	4.2 ± 1.2	-	-

[a] Measurement was performed using a filter with a cutoff of $\tilde{\nu}$ > 2000 cm^{-1}. [b] Weighted mean and standard error.

Determination of equilibrium data

Methodology of measurements/analyses

*Determining the ratio of **1/2**:* The IR intensities measured at any given time can be normalized under the use of the difference spectrum presented in Figure S1, signifying the conversion of one equivalent of benzene oxide (**1**) to one equivalent of oxepin (**2**). The intensity ratios of the peak at 772 cm^{-1} (belonging to **1**) and of the peaks at 737 and 1078 cm^{-1} (assigned to **2**) could thus be analysed and averaged to obtain the ratio of **1/2**.

Determining ΔG: Though the sample was cooled to - 40°C, the ratio determined upon deposition is assumed to be representative of the gas phase equilibrium at room temperature due to thermal equilibration with the deposition equipment on its way to the cold window. If the ratio is instead assumed to be representative of the gas phase equilibrium at - 40°, a value of $\Delta G^{233\,K}$ = - 1.17 kcal mol^{-1} results. As a sidenote, both values represent the lower limit for ΔG since tunneling during the deposition (approx. 10 minutes) cannot be accounted for, resulting in an underestimation of the ratio **1/2** and thus an increased ΔG.

Determining ΔE: After deposition, the sample was left in the IR spectrometer without filter for approx. 70 h, in order to measure kinetics. To ensure that the equilibrium was not influenced by IR irradiation, the sample was then removed from the spectrometer and kept in the dark, apart from the final IR measurement (duration < 10 minutes). Due to the kinetics' high dispersivity it is doubtful whether the ratio determined from the long-term experiment actually represents the $\Delta E^{0\,K}$ as the reaction might not fully proceed in solid argon (making ΔE an upper limit). However, the ratio determined via the IR intensities at the "end" of the reaction agrees well with the ratio obtained via the constant c in eq. 1, signifying the extrapolated intensities at "infinite" times.

Calculated complexes

General methodology for quantumchemical calculations

All gas-phase DFT geometry optimizations and frequency calculations were carried out using the M06-2X functional[2] and the D3 dispersion correction,[3] while employing the def2-TZVP basis set.[4] DFT and CCSD(T) calculations were performed with the programs Gaussian 09[5] and Molpro 2012,[6] respectively.

Methodology for systematic calculation of complexes

To investigate the energetics of the respective 1 : 1 complexes between $BrCF_3$, ICF_3 or H_2O and benzene oxide (**1**) or oxepin (**2**), 100 randomly assembled geometries were systematically calculated via the multiple minima hypersurface (MMH) procedure[7] (box size = 6 Å) at the M06-2X-d3/def2-TZVP level of theory. The respective most energetically stable complexes found by this methodology (with a cutoff of $\Delta E < 1.5$ kcal mol^{-1} with regards to the most stable one) are depicted below.

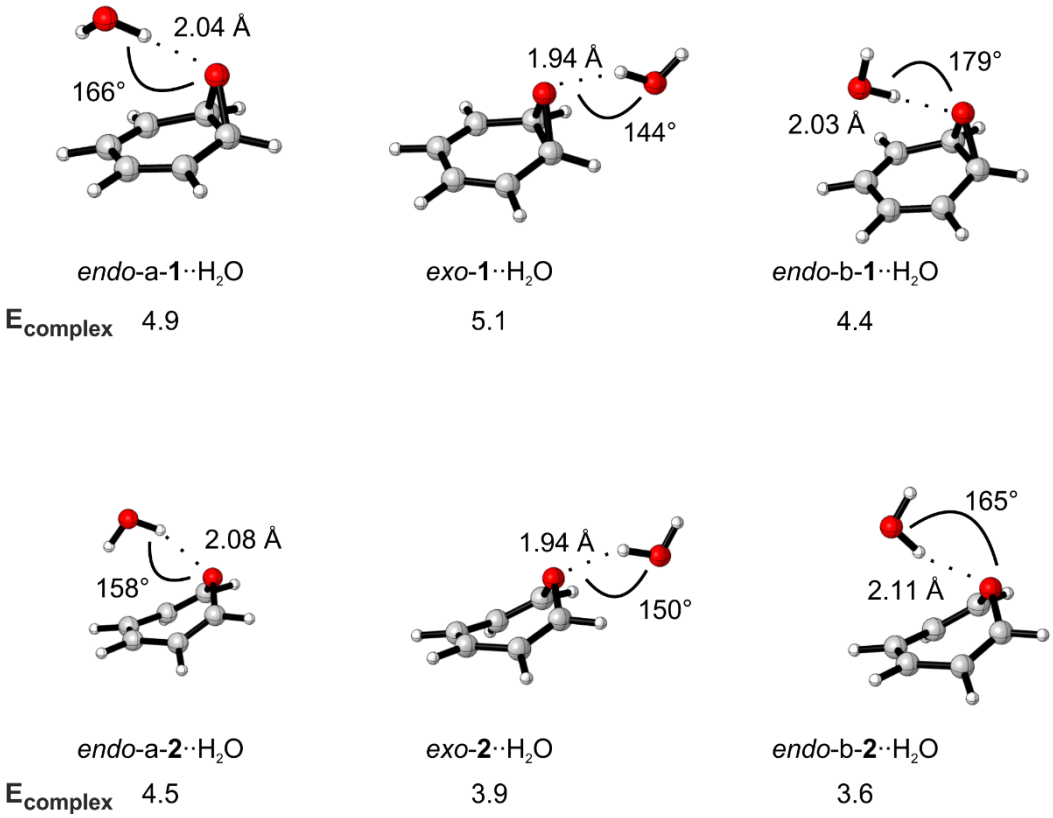

	endo-a-**1**··H_2O	*exo*-**1**··H_2O	*endo*-b-**1**··H_2O
$E_{complex}$	4.9	5.1	4.4
	endo-a-**2**··H_2O	*exo*-**2**··H_2O	*endo*-b-**2**··H_2O
$E_{complex}$	4.5	3.9	3.6

Figure S3. All complexes of **1** and **2** with H_2O found by the MMH procedure and subsequent optimization at the M06-2X-d3/def2-TZVP level of theory.

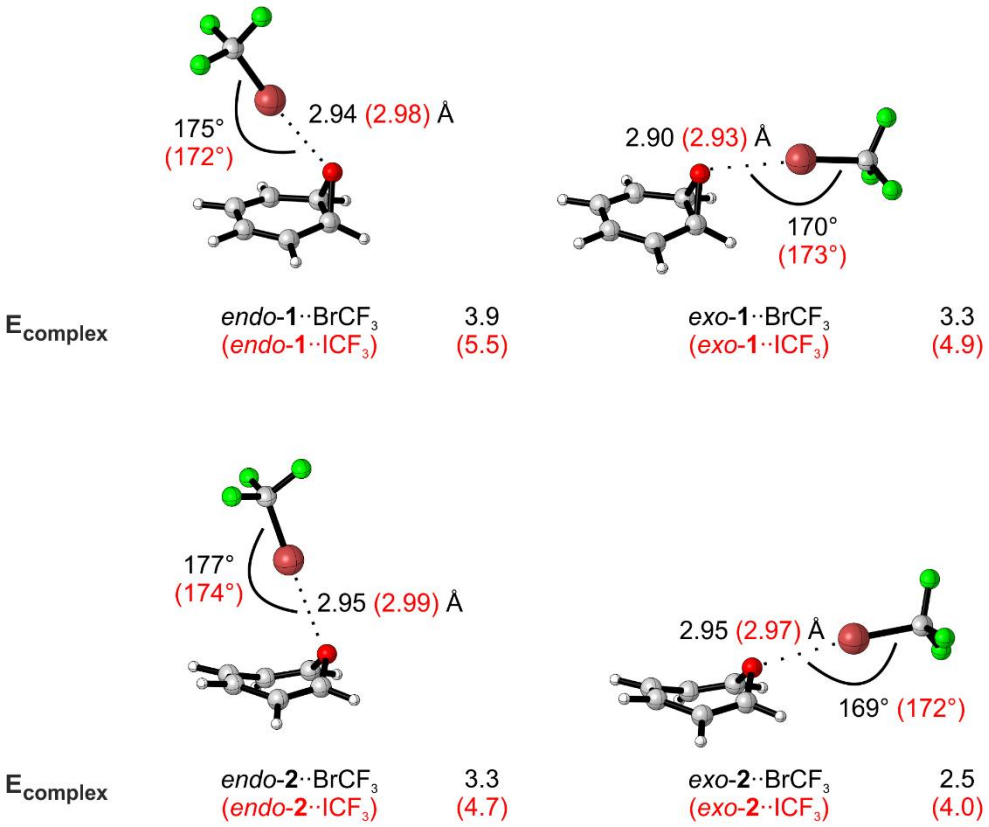

Figure S4. All complexes of **1** and **2** with $BrCF_3$ and ICF_3 found by the MMH procedure and subsequent optimization at the M06-2X-d3/def2-TZVP level of theory.

Synthesis

All synthetic procedures were taken from literature,[8] with the obtained NMR data for the products matching the ones reported previously.

1,2-Epoxy-cyclohex-4-ene

To a solution of 2.3 mL (2.0 g, 25.0 mmol) of 1,4-cyclohexadiene in 40 mL of DCM was added a suspension of 6.0 g (≈ 24 - 26 mmol) of mCPBA in 20 mL of DCM in one portion at 0°C. After stirring at rt for 5 h, the reaction mixture was filtered and the solid washed with 4 x 5 mL of DCM. The combined organic extracts were washed with 2 x 25 mL of sat. aq. Na_2SO_3 (peroxide test negative), 50 mL of sat. $NaHCO_3$ (pH ~ neutral) and 50 mL of sat. aq. NaCl. Drying over Na_2SO_4, filtration and evaporation of the solvent resulted in 1.4 g (14.2 mmol, 58% yield) of 1,2-epoxy-cyclohex-4-ene as colourless liquid.

^{1}H-NMR (200 MHz, $CDCl_3$): δ = 5.44 (“p”, *J* = 1.2 Hz, 2H), 3.24 (dq, *J* = 2.1, 1.1 Hz, 2H), 2.72 – 2.25 (m, 4H) ppm.

1,2-Epoxy-4,5-dibromocyclohexane

A solution of 0.75 mL of Br_2 (2.34 g, 14.6 mmol) in 5 mL of DCM/$CHCl_3$ (1:1, v/v) was added dropwise to a solution of 1.35 g (14.0 mmol) of 1,4-cyclohexene oxide in 30 mL of DCM/$CHCl_3$ (1:1, v/v) at -70°C, at such a rate that the reaction mixture remained (pale) yellow; when the colour changed to dark orange, the addition of the bromine solution was stopped. The reaction mixture was stirred at -70°C for 30 min, then allowed to warm to rt. 15 mL of sat. aq. $Na_2S_2O_4$ were added and the aqueous layer was extracted with 3 x 15 mL of DCM. Drying over Na_2SO_4, filtration and evaporation of the solvent resulted in 3.30 g (12.9 mmol, 92% yield) of 1,2-epoxy-4,5-dibromocyclohexane as colourless crystalline solid.

^{1}H-NMR (300 MHz, $CDCl_3$): δ = 4.30 (ddd, *J* = 7.7, 6.6, 4.6 Hz, 1H), 4.26 – 4.13 (m, 1H), 3.27 – 3.21 (m, 2H), 3.00 (ddt, *J* = 16.1, 4.6, 1.1 Hz, 1H), 2.90 (ddd, *J* = 16.5, 6.3, 3.5 Hz, 1H), 2.65 (br dd, *J* = 16.5, 6.3 Hz, 1H), 2.46 (dddd, *J* = 16.0, 6.7, 3.5, 0.7 Hz, 1H,) ppm.

Benzene oxide/oxepin (**1/2**)

1.15 g (4.5 mmol) of epoxy-4,5-dibromocyclohexane were dissolved in 25 mL of dry ether and cooled to 0°C before addition of 1.0 g (8.9 mmol) of KO*t*Bu in four portions over the course of one hour. After stirring for 1.5 h at rt, the reaction mixture was poured into 50 mL of H_2O. After addition of 25 mL of ether, the organic solution was washed with 25 mL of H_2O, 50 mL of sat. $NaHCO_3$ and 50 mL of sat. aq. NaCl. Drying over $MgSO_4$, filtration and evaporation of the solvent resulted in 0.32 g (3.4 mmol, 76% yield) of oxepin/benzene oxide as yellow liquid.

^{1}H-NMR (200 MHz, $CDCl_3$): δ = 6.26 (ddt, *J* = 4.7, 2.8, 0.7 Hz, 2H), 5.93 (tdd, *J* = 4.9, 2.5, 1.1 Hz, 2H), 5.12 (dt, *J* = 4.8, 0.8 Hz, 2H) ppm.

Z-Matrices

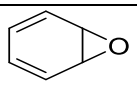 **1** CCSD(T)/def2-TZVP E = -306.752497	C	-0.1131564249	1.4400241344	0.7278681012
	C	-0.1131564249	1.4400241344	-0.7278681012
	C	0.1832239040	0.3238595239	-1.4337332516
	C	0.1832239040	0.3238595239	1.4337332516
	C	0.3254735785	-0.9738534711	-0.7523447909
	C	0.3254735785	-0.9738534711	0.7523447909
	H	-0.2553110450	2.3858418663	1.2426570853
	H	-0.2553110450	2.3858418663	-1.2426570853
	H	0.3273862551	0.3643794566	-2.5094440715
	H	0.3273862551	0.3643794566	2.5094440715
	H	0.8465956811	-1.7720993036	-1.2767828251
	H	0.8465956811	-1.7720993036	1.2767828251
	O	-0.8076522377	-1.4355521431	0.0000000000

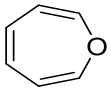 **2** CCSD(T)/def2-TZVP E = -306.753909	C	-0.1541108256	-1.4344247291	-0.6775542635
	C	-0.1541108256	-1.4344247291	0.6775542635
	C	0.2604610137	-0.3014526937	1.4973778712
	C	0.2604610137	-0.3014526937	-1.4973778712
	C	0.1216327708	0.9872565427	1.1461994166
	C	0.1216327708	0.9872565427	-1.1461994166
	H	-0.4017093922	-2.3567488688	-1.1974565657
	H	-0.4017093922	-2.3567488688	1.1974565657
	H	0.7263483515	-0.5027153355	2.4585813725
	H	0.7263483515	-0.5027153355	-2.4585813725
	H	0.4754487914	1.8121853752	1.7596235924
	H	0.4754487914	1.8121853752	-1.7596235924
	O	-0.5534251689	1.3906371782	0.0000000000

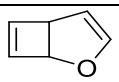	C	0.95770900	1.15067700	-0.06794200
	C	1.58753300	0.02246200	-0.37608600
M06-2X-D3/def2-TZVP	O	0.96806000	-1.13191600	0.00223500
E = -307.258707	H	1.32420400	2.14225900	-0.27715900
	H	2.53040600	-0.11963000	-0.88386500
	C	-0.29418400	-0.75731500	0.56594800
	H	-0.43993100	-1.30683700	1.49451200
	C	-0.34710700	0.80926200	0.59632300
	H	-0.52454000	1.30757700	1.55042300
	C	-1.44648400	-0.68401400	-0.40329800
	H	-1.97671900	-1.44795900	-0.95577200
	C	-1.53515600	0.64408700	-0.33862400
	H	-2.19177300	1.36896200	-0.80393700

	C	0.00000000	0.00000000	-1.17383900
ICF_3	I	0.00000000	0.00000000	0.96712400
M06-2X-D3/def2-TZVP	F	0.00000000	1.23929700	-1.63757500
E = -635.281973	F	1.07326300	-0.61964900	-1.63757500
	F	-1.07326300	-0.61964900	-1.63757500

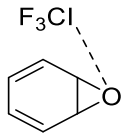	C	2.59211400	1.55148800	0.70773800
	C	2.60332400	1.53029200	-0.74209100
	C	2.98310500	0.43963400	-1.42462400
endo-**1**••ICF_3	C	2.96017600	0.48118400	1.42775200
M06-2X-D3/def2-TZVP	H	2.38480300	2.49126300	1.20340100
E = -942.571799	H	2.40295600	2.45495500	-1.26804800
	H	3.15594400	0.48014000	-2.49218900
	H	3.11593700	0.55313400	2.49634500
	C	3.17955800	-0.81252100	0.77657500
	H	3.73223400	-1.57493700	1.31304300

	C	3.19236100	-0.83434200	-0.73238600
	H	3.75377600	-1.61165700	-1.23754800
	O	2.09821900	-1.33833000	0.02035500
	I	-0.68519600	-0.28642000	-0.01047900
	C	-2.77187900	0.18518300	0.00554300
	F	-3.18765800	0.46840900	1.23600900
	F	-3.49626300	-0.83407600	-0.44329500
	F	-3.03258700	1.23772100	-0.76310200

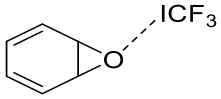

exo-**1**••ICF_3

M06-2X-D3/def2-TZVP

E = -942.570870

	C	-4.81372600	-0.66816900	-0.13094900
	C	-4.76428300	0.78089000	-0.15257300
	C	-3.67112600	1.45141000	0.23914700
	C	-3.76852600	-1.40034900	0.28121300
	C	-2.41902500	0.73839200	0.50338300
	C	-2.46996900	-0.76777700	0.52534300
	H	-5.75869700	-1.15038200	-0.34669700
	H	-5.67414700	1.31977000	-0.38423200
	H	-3.69445400	2.52316000	0.38729800
	H	-3.86591500	-2.46325500	0.46011000
	H	-1.64860100	1.23951900	1.08012000
	H	-1.73489800	-1.30276700	1.11744900
	O	-1.89902400	-0.04896800	-0.56031800
	C	3.10752600	0.03113200	0.19141500
	F	3.38558500	-0.72970900	1.24353600
	F	3.48897900	1.27188100	0.47180200
	F	3.83675100	-0.40064200	-0.82979600
	I	1.01814800	-0.03851400	-0.27440100

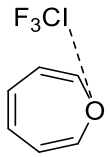

endo-**2**••ICF_3

M06-2X-D3/def2-TZVP

E = -942.570614

C	-2.77958100	1.53651600	-0.61269700
C	-2.78074300	1.48008300	0.73000200
C	-3.09601000	0.29151900	1.50416700
C	-3.09270500	0.41689200	-1.48425900
C	-2.85339500	-0.95337300	1.10339300
C	-2.84951600	-0.85687600	-1.18907200
H	-2.61389300	2.49604600	-1.08834500
H	-2.61495100	2.39632200	1.28437700
H	-3.57241100	0.41716500	2.46888500
H	-3.56783100	0.62200600	-2.43583900
H	-3.13368300	-1.83551600	1.66583500
H	-3.12820700	-1.68916300	-1.82364100
O	-2.14255400	-1.22884800	-0.05527000
I	0.68614500	-0.25896000	0.00064100
C	2.77417600	0.20789400	0.00132300
F	3.49127500	-0.81621300	0.44939800
F	3.03067300	1.25483000	0.77750300
F	3.19720200	0.49614500	-1.22470600

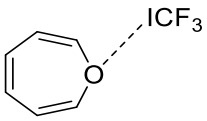

exo-**2**••ICF_3

M06-2X-D3/def2-TZVP

E = -942.569565

C	-4.78828200	-0.62942100	-0.27302500
C	-4.75511800	0.71362700	-0.27693500
C	-3.68852700	1.51097300	0.30439400
C	-3.76226800	-1.47536800	0.31304800
C	-2.41601400	1.13167300	0.36880500
C	-2.47256400	-1.15897000	0.37580800
H	-5.67470200	-1.12497200	-0.65133000
H	-5.61624900	1.25018400	-0.65788400
H	-3.93970200	2.47418700	0.73158900
H	-4.06152600	-2.42220300	0.74594300
H	-1.63545500	1.70756200	0.85299400

	H	-1.72152600	-1.77003100	0.86351200
	O	-1.96122800	-0.02744600	-0.24304600
	C	3.13145200	0.01997300	0.11602500
	F	3.46234900	-0.66496200	1.20328500
	F	3.55724700	1.26728200	0.27090300
	F	3.77559000	-0.50967300	-0.91535200
	I	1.01302300	-0.02648900	-0.19884300

	C	0.00000000	0.00000000	-0.81211200
$BrCF_3$	F	0.00000000	1.23879600	-1.26912400
	F	1.07282900	-0.61939800	-1.26912400
M06-2X-D3/def2-TZVP	F	-1.07282900	-0.61939800	-1.26912400
E = -2911.848378	Br	0.00000000	0.00000000	1.11825800

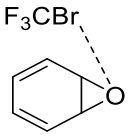	C	2.29100000	1.52132100	0.71577500
	C	2.32247400	1.51091700	-0.73347700
	C	2.75903600	0.44268500	-1.41778000
endo-**1**••$BrCF_3$	C	2.69683400	0.46320700	1.43362300
M06-2X-D3/def2-TZVP	H	2.03634900	2.44747900	1.21510500
E = -3219.135756	H	2.08972500	2.42964100	-1.25661500
	H	2.94517200	0.49959700	-2.48247200
	H	2.83594400	0.53536200	2.50462200
	C	2.98328900	-0.81513400	0.77751400
	H	3.56729900	-1.55242800	1.31640000
	C	3.01667600	-0.82588300	-0.73153200
	H	3.62398900	-1.57040700	-1.23350000
	O	1.93990100	-1.38525700	0.00350900
	C	-2.67241700	0.13041400	0.00196300
	F	-3.05031700	0.48265400	1.22261200

	F	-3.43885600	-0.87472300	-0.39400200
	F	-2.88690900	1.15702000	-0.80869700
	Br	-0.81755200	-0.37591200	-0.01563800

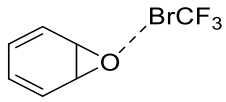

exo-**1**••$BrCF_3$

M06-2X-D3/def2-TZVP

E = -3219.134683

C	-4.52713800	-0.71400800	-0.06463900
C	-4.51780800	0.73566200	-0.07109900
C	-3.41651000	1.43150500	0.24741600
C	-3.43500100	-1.42130500	0.26021500
C	-2.12869400	0.75177500	0.40410600
C	-2.13839300	-0.75711700	0.41095000
H	-5.47313000	-1.21873400	-0.21450900
H	-5.45721100	1.25122100	-0.22532200
H	-3.45874600	2.50006300	0.41409300
H	-3.49133900	-2.48774500	0.43607500
H	-1.33066500	1.26653500	0.92873500
H	-1.34683700	-1.27723300	0.94014200
O	-1.67217500	-0.01068600	-0.70235200
C	3.05161900	0.00638900	0.17538800
F	3.24232800	-0.82399700	1.18907800
F	3.40806400	1.22181400	0.56054300
F	3.83964700	-0.36394800	-0.82033400
Br	1.20561500	-0.01288200	-0.37708600

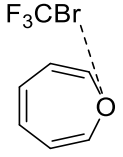

endo-**2**••$BrCF_3$

M06-2X-D3/def2-TZVP

E = -3219.134865

C	-2.47209000	1.52114500	-0.62388400
C	-2.47766800	1.47547100	0.71845800
C	-2.85005700	0.30878700	1.50131400
C	-2.83739800	0.41034900	-1.48720300
C	-2.67070800	-0.95017500	1.11118000
C	-2.66037900	-0.87210200	-1.18226200
H	-2.25810500	2.46701300	-1.10765400

	H	-2.26663300	2.38615200	1.26670300
	H	-3.31852600	0.46470600	2.46554700
	H	-3.29827900	0.63124100	-2.44231400
	H	-2.99385000	-1.80957300	1.68637300
	H	-2.97844900	-1.69055900	-1.81681800
	O	-1.98192100	-1.27868800	-0.04489600
	C	2.66862000	0.16275800	0.00100800
	F	3.43559200	-0.84166700	0.39669000
	F	2.87066000	1.18470300	0.81944400
	F	3.05224800	0.52342900	-1.21463400
	Br	0.81545100	-0.35300100	0.00177600

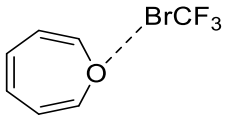

exo-**2**••$BrCF_3$

M06-2X-D3/def2-TZVP

E = -3219.133757

C	-4.53740200	-0.65335700	-0.06378500
C	-4.52316500	0.68955000	-0.06981200
C	-3.38140900	1.50084800	0.31822700
C	-3.41309100	-1.48520700	0.33182600
C	-2.11122600	1.13907700	0.16341800
C	-2.13553200	-1.15198800	0.17388000
H	-5.46841200	-1.16155400	-0.28614800
H	-5.44319100	1.21529000	-0.29702600
H	-3.56682000	2.46298400	0.78019600
H	-3.61903600	-2.43881200	0.80261500
H	-1.27091700	1.73399100	0.50352900
H	-1.30798100	-1.76129000	0.51973100
O	-1.74304400	-0.01360500	-0.51136600
C	3.06411300	0.00872900	0.16263300
F	3.28243100	-0.80546400	1.18242200
F	3.42896600	1.23014800	0.51696500
F	3.82120500	-0.37750800	-0.85006000
Br	1.20153000	-0.01863600	-0.33355000

H_2O	O	0.00000000	0.00000000	0.11619900
M06-2X-D3/def2-TZVP	H	0.00000000	0.76434100	-0.46479500
E = -76.404569	H	0.00000000	-0.76434100	-0.46479500

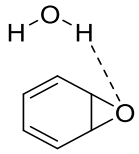 *endo*-a-**1**••H_2O M06-2X-D3/def2-TZVP E = -3219.135756				
	C	0.29756400	1.31417100	-0.82107400
	C	-0.05595200	1.52832400	0.56856000
	C	-0.89868800	0.70639400	1.21067900
	C	-0.19194100	0.27813400	-1.51985300
	C	-1.31933300	-0.55621800	0.59723500
	C	-0.94066200	-0.78638800	-0.84468900
	H	0.87810900	2.07845400	-1.32306400
	H	0.29221100	2.43239500	1.05082500
	H	-1.29193700	0.96089800	2.18628500
	H	-0.06804200	0.21946900	-2.59370200
	H	-2.19681100	-1.05591500	0.99098400
	H	-1.55645300	-1.44401400	-1.44700900
	O	-0.28667300	-1.45663700	0.22248200
	O	2.57759600	-0.66141000	0.49848200
	H	2.60688500	-0.18648700	-0.33557100
	H	1.66272600	-0.96692800	0.55839700

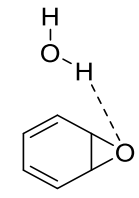 *endo*-b-**1**••H_2O M06-2X-D3/def2-TZVP E = -383.692658				
	C	-0.21625700	1.38145500	0.75481700
	C	-0.15649500	1.43224700	-0.69289800
	C	0.59756400	0.57376400	-1.39461600
	C	0.47972200	0.47353600	1.45427900
	C	1.21454000	-0.58044200	-0.73541300
	C	1.15241700	-0.63333600	0.76908300
	H	-0.76183000	2.16061200	1.27068100

	H	-0.65976600	2.24746600	-1.19601100
	H	0.77031200	0.71607400	-2.45341000
	H	0.56277100	0.53988600	2.53128700
	H	2.02322100	-1.09464100	-1.24166300
	H	1.91852900	-1.18367700	1.30275500
	O	0.33768500	-1.46575600	-0.04837500
	O	-2.54168600	-0.64688800	-0.06060500
	H	-3.03829400	-1.45443600	-0.20986800
	H	-1.61187200	-0.91347700	-0.06344700

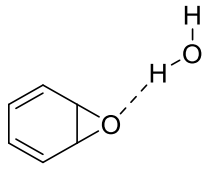

exo-**1**••H_2O

M06-2X-D3/def2-TZVP

E = -383.693855

	C	-2.09566000	0.72493300	0.09450700
	C	-2.09561500	-0.72501800	0.09449000
	C	-0.98661000	-1.42599200	-0.18374100
	C	-0.98670300	1.42598400	-0.18373000
	C	0.31028500	-0.75398900	-0.28891900
	C	0.31022400	0.75407200	-0.28895800
	H	-3.04377000	1.23510300	0.20886900
	H	-3.04369800	-1.23524800	0.20881800
	H	-1.02916100	-2.49335600	-0.35799600
	H	-1.02932900	2.49334700	-0.35797200
	H	1.13126400	-1.26183100	-0.78213700
	H	1.13119800	1.26195800	-0.78212900
	O	0.72491700	0.00002100	0.84595400
	O	3.31898300	-0.00002000	-0.15085500
	H	4.16223500	0.00012500	0.30604800
	H	2.63454800	-0.00003900	0.53382300

	C	-0.31888600	1.43227500	-0.67208600
	C	-0.31875100	1.43218900	0.67231200
	C	-0.76111600	0.31863300	1.49534800

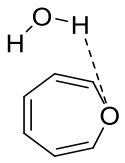

endo-a-**2**••H_2O

M06-2X-D3/def2-TZVP

E = -383.693083

C	-0.76141500	0.31882500	-1.49517600
C	-0.66987200	-0.96173200	1.14816600
C	-0.67009800	-0.96158500	-1.14817800
H	-0.05610400	2.34816200	-1.18897500
H	-0.05586700	2.34801000	1.18926600
H	-1.20934300	0.53780600	2.45664700
H	-1.20983500	0.53812300	-2.45635600
H	-1.04498000	-1.77742400	1.75414300
H	-1.04532800	-1.77719800	-1.75418500
O	-0.01333700	-1.37626300	-0.00009800
O	2.69014600	-0.09015300	-0.00022400
H	2.24764900	0.76301000	-0.00016800
H	1.96016300	-0.72078200	-0.00010200

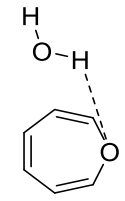

endo-b-**2**••H_2O

M06-2X-D3/def2-TZVP

E = -383.691735

C	0.24728300	1.39356500	0.74386100
C	0.45537700	1.43957900	-0.58344800
C	1.02373400	0.35363500	-1.36401200
C	0.56079900	0.25168900	1.58590900
C	0.85524500	-0.93453100	-1.07923700
C	0.50092100	-1.01269400	1.17784900
H	-0.10922300	2.28742200	1.24142400
H	0.25936200	2.36911500	-1.10417300
H	1.63028500	0.59964900	-2.22704100
H	0.87049200	0.43280900	2.60791800
H	1.31703300	-1.74547100	-1.62921700
H	0.77846700	-1.86371600	1.78757700
O	-0.00398300	-1.34921000	-0.07087400
O	-2.69810100	0.08676600	-0.29503000
H	-3.20916300	-0.71949800	-0.39651100
H	-1.78073600	-0.20820700	-0.23828200

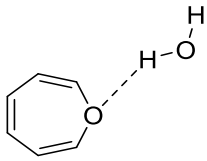 *exo*-**2**••H_2O M06-2X-D3/def2-TZVP E = -383.692100	C	2.09455100	0.67904800	-0.15533500
	C	2.10150600	-0.66515600	-0.15504900
	C	0.98239800	-1.49128900	0.26345600
	C	0.96704700	1.49415300	0.26222900
	C	-0.29534400	-1.14807600	0.12993500
	C	-0.30724100	1.13832600	0.12853200
	H	3.01448700	1.19966000	-0.39449500
	H	3.02669700	-1.17651400	-0.39387700
	H	1.19242200	-2.44181400	0.73859200
	H	1.16740000	2.44740800	0.73607800
	H	-1.12972800	-1.73033900	0.50398200
	H	-1.14783700	1.71301300	0.50044000
	O	-0.67441700	-0.00734600	-0.56633100
	O	-3.40402000	0.00705500	0.11489100
	H	-4.14661500	-0.04397600	-0.49047700
	H	-2.60683500	-0.00714500	-0.43132800

Literature references

[1] W. Siebrand, T. A. Wildman, *Acc. Chem. Res.* **1986**, *19*, 238-243.

[2] Y. Zhao, D. G. Truhlar, *Acc. Chem. Res.* **2008**, *41*, 157-167.

[3] S. Grimme, J. Antony, S. Ehrlich, H. Krieg, *J. Chem. Phys.* **2010**, *132*, 154104.

[4] F. Weigend, R. Ahlrichs, *Phys. Chem. Chem. Phys.* **2005**, *7*, 3297-3305.

[5] M. J. Frisch, G. W. Trucks, H. B. Schlegel, G. E. Scuseria, M. A. Robb, J. R. Cheeseman, G. Scalmani, V. Barone, G. A. Petersson, H. Nakatsuji, X. Li, M. Caricato, A. V. Marenich, J. Bloino, B. G. Janesko, R. Gomperts, B. Mennucci, H. P. Hratchian, J. V. Ortiz, A. F. Izmaylov, J. L. Sonnenberg, Williams, F. Ding, F. Lipparini, F. Egidi, J. Goings, B. Peng, A. Petrone, T. Henderson, D. Ranasinghe, V. G. Zakrzewski, J. Gao, N. Rega, G. Zheng, W. Liang, M. Hada, M. Ehara, K. Toyota, R. Fukuda, J. Hasegawa, M. Ishida, T. Nakajima, Y. Honda, O. Kitao, H. Nakai, T. Vreven, K. Throssell, J. A. Montgomery Jr., J. E. Peralta, F. Ogliaro, M. J. Bearpark, J. J. Heyd, E. N. Brothers, K. N. Kudin, V. N. Staroverov, T. A. Keith, R. Kobayashi, J. Normand, K. Raghavachari, A. P. Rendell, J. C. Burant, S. S. Iyengar, J. Tomasi, M. Cossi, J. M. Millam, M. Klene, C. Adamo, R. Cammi, J. W. Ochterski, R. L. Martin, K. Morokuma, O. Farkas, J. B. Foresman, D. J. Fox, Wallingford, CT, **2009**.

[6] H.-J. Werner, P. J. Knowles, G. Knizia, F. R. Manby, M. Schütz, *Wiley. Interdiscip. Rev. Comput. Mol. Sci.* **2012**, *2*, 242-253.

[7] L. A. Montero, A. M. Esteva, J. Molina, A. Zapardiel, L. Hernandez, H. Marquez, A. Acosta, *J. Am. Chem. Soc.* **1998**, *120*, 12023-12033.

[8] aA. Ravi, P. S. Krishnarao, T. A. Shumilova, V. N. Khrustalev, T. Rüffer, H. Lang, E. A. Kataev, *Org. Lett.* **2018**, *20*, 6211-6214; bS. Da Silva Pinto, S. G. Davies, A. M. Fletcher, P. M. Roberts, J. E. Thomson, *Org. Lett.* **2019**, *21*, 7933-7937; cJ. R. Gillard, M. J. Newlands, J. N. Bridson, D. J. Burnell, *Can. J. Chem.* **1991**, *69*, 1337-1343.